Extensional rheometry of magnetic dispersions

F. J. Galindo-Rosales[a)]

Centro de Estudos de Fenómenos de Transporte (CEFT), Dep. de Engenharia Química, Faculdade de Engenharia da Universidade do Porto, Rua Dr. Roberto Frias s/n, 4200-465 Porto, Portugal

J. P. Segovia-Gutiérrez

Dep. de Física Aplicada, Facultad de Ciencias, Avda. Fuente nueva s/n, 18071 Granada, Spain

F. T. Pinho

Centro de Estudos de Fenómenos de Transporte (CEFT), Dep. de Engenharia Mecânica, Faculdade de Engenharia da Universidade do Porto, Rua Dr. Roberto Frias s/n, 4200-465 Porto, Portugal

M. A. Alves

Dep. de Engenharia Química (CEFT), Faculdade de Engenharia da Universidade do Porto, Rua Dr. Roberto Frias s/n, 4200-465 Porto, Portugal

J. de Vicente

Dep. de Física Aplicada, Facultad de Ciencias, Avda. Fuente nueva s/n, 18071 Granada, Spain

(Received 1 July 2014; final revision received 7 November 2014; published 12 December 2014)

Synopsis

This work presents a technique and develops an apparatus that allows the application of homogeneous external magnetic fields (parallel or perpendicular to the deformation axis) to a fluid sample undergoing extensional flow kinematics while measuring the filament thinning using the commercial version of the capillary breakup extensional rheometer (Haake™ CaBER™ 1, Thermo Scientific). We also present innovative rheological measurements of several commercial ferrofluids (FFs) and one magnetorheological fluid (MRF) under uniaxial extensional flow. The experimental results demonstrate that FFs exhibit a Newtonian-like behavior in the absence of magnetic fields. When a magnetic field is applied perpendicular to the extensional flow, no significant effects are observed similar to shear experiments. However, when the external magnetic field is aligned with the extensional flow, the filament takes longer to break up but otherwise behaves as a Newtonian fluid. In

[a)]Author to whom correspondence should be addressed; electronic mail: galindo@fe.up.pt

the case of the MRF, due to the higher concentration of particles and larger particle size, the differences in the extensional behaviors are much more dramatic regardless of the orientation of the magnetic field compared to the case when no magnetic field is applied.
[http://dx.doi.org/10.1122/1.4902356]

I. INTRODUCTION

Colloidal dispersions with at least one magnetic field-responsive phase experience dramatic changes in their properties (rheological, magnetic, electrical, thermal, acoustic, and other mechanical and physical properties) when exposed to magnetic fields. In most cases, it is the particulate phase that responds to the field [e.g., magneto-rheological fluids and ferrofluids (FFs)], but there are also cases where it is the carrier fluid that is sensitive to the field (e.g., inverse FFs) [de Vicente (2013)]. Hereafter, these colloidal dispersions will be referred to as magnetic fluids.

Magnetic fluids are complex smart materials where magnetic body forces appear when they are magnetized with an external magnetic field, and may exhibit a transition from liquidlike to solidlike behavior in a fraction of a millisecond for a sufficiently large magnetic field. This liquid-to-solid transition provides an efficient way to control force or torque transmission in applications dealing with actuation, damping, etc. [Jacob (1951); Bossis *et al.* (2002); Huang *et al.* (2002); Gerlach *et al.* (2009); Bose *et al.* (2013)]. In order to correctly predict the behavior of these fluids and to widen their applicability, it is essential to know the relationship between the in-flow behavior and the external applied magnetic field.

Experiments under controlled shear and elongational flows are typically used in the field of rheology in order to measure material functions of non-Newtonian fluids and to subsequently obtain an appropriate constitutive equation [Morrison (2001)]. Traditionally, the devices used to quantify the effect of a magnetic field on the rheology of magnetic fluids are rotational rheometers conveniently adapted with either coils and/or magnetic circuits, which impose magnetic fields on the sheared sample [Ocalan and McKinley (2013)]. The configuration of coils depends on the space available around the rotating measuring device. A pair of coils in Helmholtz configuration allows one to impose a well-defined field on a large volume and minimizes field gradients, but the maximum magnetic field strength attainable is small (approx. 1 kA/m). Using a single coil around the rotating device allows one to reach larger magnetic fields (approx. 10 kA/m), but the temperature must remain within a specified range for an extended period of time, and it is difficult to ensure that the gap between the measuring surfaces is correctly filled with the fluid to be measured [Bossis *et al.* (2002)]. To apply magnetic fields above 100 kA/m ($\approx$1000 Oe) a magnetic circuit is needed. In this case, the field can either be parallel to the axis of rotation of parallel-plate geometries with the polar pieces having the same axis of symmetry, or the field can be radial everywhere, and thus perpendicular to the flowlines [Shulman *et al.* (1986)] in a cylindrical Couette cell. In the latter configuration, the field is not constant throughout the gap [Laun *et al.* (1996)] which promotes particle migration toward the inner wall where the magnetic field is greater; this results in a viscosity gradient. Furthermore, the height of the cylinder must be smaller than its radius in order to avoid the magnetic saturation of the central iron rod and this can introduce significant end effects. Thus, in practice, the parallel-plate and the cone-plate geometries are the preferred measuring devices for high magnetic field rheological measurements in shear flow [de Gans *et al.* (1999)]. In the cone-plate geometry, the shear rate is constant throughout the suspension but the variable fluid thickness can induce a variable structure within the fluid sample. In the parallel-plate geometry, the gap is constant and easy to change, which allows for the reduction of wall slip by the use of serrated

surfaces, or at least its quantification using Mooney's correction, but on the other hand the shear rate is not constant within the sample [Morrison (2001)].

It is not surprising that the rheological properties of magnetic fluids under shearing flows (steady, transient, small amplitude oscillatory shear flow-SAOS-, large amplitude oscillatory shear flow-LAOS-, etc.) have been extensively investigated. Shearing flows are very useful from a practical point of view, since in diverse applications such as servo-valves, dampers, and shock absorbers, the magnetic fluid is subjected to a Poiseuille flow between fixed poles (known as valve or pressure driven flow mode), whereas in other applications, such as brakes, clutches, and chucking/locking devices, the magnetic fluid undergoes Couette flow between two relatively moveable poles (known as direct-shear mode) [Olabi and Grunwald (2007); de Vicente *et al*. (2011a)]. These configurations are shown in Figs. 1(a) and 1(b), respectively, which include the schematic representations of the magnetic field lines, velocity field, and shear rate, as well as the corresponding analytical solution for the flow kinematics assuming a constant viscosity fluid.

In some applications, such as in small amplitude vibration dampers, the mode of operation configures a biaxial elongational flow (known as squeeze mode) [Olabi and Grunwald (2007)]. However, very little information exists on this issue in the literature despite reports or suggestions that the yield stress that could be achieved in extensional flow would be up to ten times larger than the achievable yield stress with either of the two shearing flow modes mentioned above [de Vicente *et al*. (2011a)]. Among the few attempts to characterize the rheology of magnetic fluids in elongational flow, there are some preliminary squeeze flow experiments using the parallel-plate geometry [cf. Fig. 1(c)] in a standard shear rheometer with slow approaching speeds between the parallel-plates [de Vicente *et al*. (2011b); Ruiz-López *et al*. (2013); Guo *et al*. (2013a);

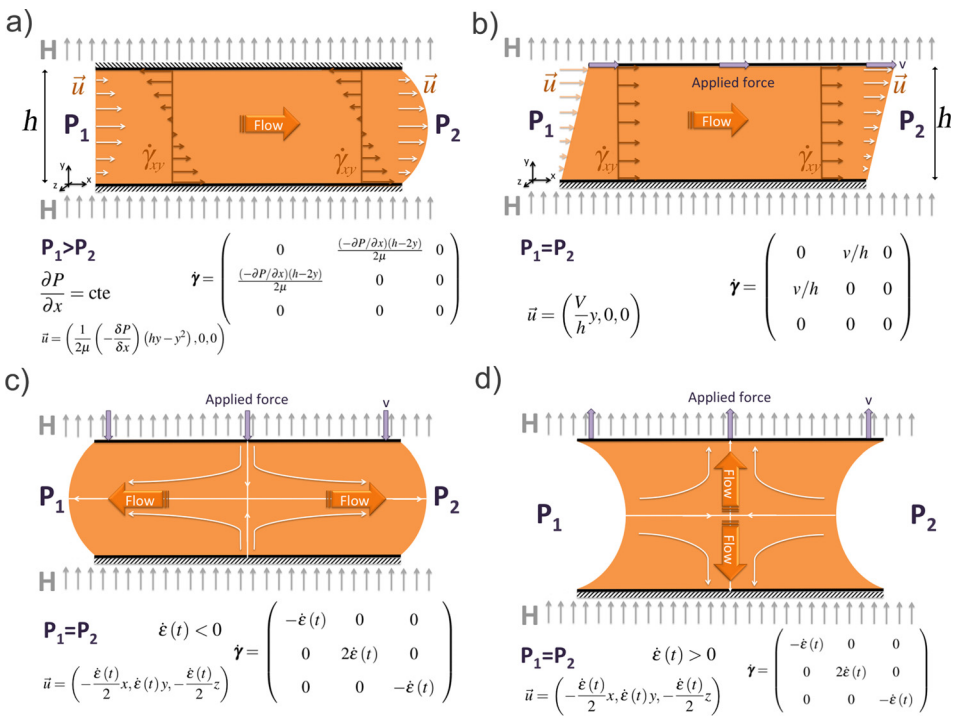

FIG. 1. Basic flow kinematics: (a) pressure driven shear flow, (b) direct-shear flow, (c) ideal biaxial stretching flow, and (d) ideal uniaxial elongational flow.

Guo *et al*. (2013b)]. However, it must be noted that in real squeeze flow the fluid is simultaneously subjected to shear and extensional flow deformations due to no slip at the walls, thus the flow kinematics is purely extensional only at the stagnation point [Haward *et al*. (2013)]. It is also important to highlight here that in the three modes mentioned above, the magnetic field is perpendicular to the flow field. However, whereas in the valve and direct-shear modes, the elongated structures created by the action of the magnetic field are subjected to shear stresses, in the squeeze mode the structures are compressed and sheared at the same time. It is this particular difference that leads to larger values of the yield stress in squeeze flow than with the two other modes. The search for new modes of operation is currently very active and as a consequence an alternative valve configuration called Magnetic Gradient Pinch has been recently proposed for controlling magnetorheological fluids (MRFs) [Gonçalves and Carlson (2009)]. This configuration consists of a contraction/expansion flow, where the fluid structures are simultaneously subjected to shear and extensional stresses. Hence, a deeper knowledge of the rheological behavior of magnetic fluids under shear-free (elongational) flow conditions [as shown in Fig. 1(d), for instance] is necessary for better control of the flow kinematics, as shear alone is insufficient to fully determine the response of a material under real complex flow conditions. Therefore, a new technique able to measure relevant material properties of magnetic fluids in uniaxial extensional flow is of considerable value.

Among the plethora of techniques developed for extensional characterization of mobile liquids, filament stretching rheometry has sparked great interest since the pioneering works of Matta and Titus (1990) and Bazilevsky *et al*. (1990). Nowadays, it is considered an accurate method for characterizing the extensional response of viscoelastic fluids [Anna *et al*. (2001); Galindo-Rosales *et al*. (2013)], and its major advantage is that the velocity field far from the rigid end plates is essentially one-dimensional and purely extensional [Schultz and Davis (1982)]. Over the past two decades, many different filament stretching configurations have been proposed for generating extensional flows, but two among those have showed enhanced performance and simplicity for rheometric purposes [McKinley *et al*. (2001); Galindo-Rosales *et al*. (2013)]:

(1) The filament stretching extensional rheometer (FiSER) imposes an exponential velocity on the upper plate in order to induce uniaxial extensional flow with constant strain rate, rather than constant tensile force, as in the original concept of Matta and Titus (1990). The temporal evolution of the tensile force exerted by the fluid column on the bottom stationary end plate and of the filament radius at the axial midplane of the filament are both measured and used to compute the transient extensional viscosity [McKinley *et al*. (2001)]. A more reliable version of the FiSER apparatus can use a real-time algorithm to control the upper plate velocity in order to achieve the desired exponential decay of the filament diameter at the midpoint [Anna *et al*. (1999)].
(2) The capillary breakup extensional rheometer (Haake CaBER 1) [Thermo Fisher Scientific (2006); Braithwaite *et al*. (2002)], based on the ideas of Bazilevsky *et al*. (1990), imposes an extensional step strain of order unity, and the filament subsequently thins under the influence of capillary forces without additional kinematic inputs at the boundaries. The fluid filament undergoes a thinning process, with an extensional strain rate dictated by the interfacial tension and extensional properties of the fluid. Large extensional strains can still be attained at the midregion of the filament as it progressively thins and eventually breaks. Typically, the only measured quantity is the time evolution of the midpoint diameter of the thinning filament, and the relaxation time of a viscoelastic liquid is determined from the exponential decay

of the filament diameter with time [McKinley *et al*. (2001)]. For a Newtonian fluid, the filament diameter decays linearly with time. While the FiSER technique is suitable to characterize viscous polymer solutions and melts, the force transducer resolution and accuracy, and gravitational and inertial effects can preclude its use with low viscosity solutions. Here, filament breakup investigations using the CaBER 1^{TM} device provide a cheaper alternative for measuring extensional properties. Monitoring the filament thinning dynamics after a rapid extensional deformation provides important information regarding the relaxation time, the non-Newtonian behaviour and the time to breakup the fluid.[1]

For all these reasons, capillary breakup rheometry is being used more frequently to investigate the extensional properties of complex fluids, such as viscoelastic fluids [McKinley (2005)], yield stress fluids [Niedzwiedz *et al*. (2009)], or shear thickening fluids [Chellamuthu *et al*. (2009); White *et al*. (2010)].

Even though both devices (FiSER and CaBER) are capable of characterizing the extensional properties of a wide range of complex fluids, neither of them supplies an external magnetic field while executing the extensional deformation and so neither of them are currently capable of characterizing the extensional behavior of magnetic fluids under the action of magnetic fields. We describe here a technique that, in general terms, allows the application of an external homogeneous magnetic field (AC or DC, constant or tuneable, and aligned or perpendicular to the flow direction) to a fluid sample undergoing uniaxial extensional flow kinematics in the commercial version of the Capillary Breakup Extensional Rheometer (Haake^{TM} CaBER 1^{TM}, Thermo Scientific) [Braithwaite *et al*. (2002)]. We describe two embodiments of this technique applied to the CaBER 1^{TM} device, and we show results of measurements of the extensional properties of some commercial magnetic fluids under the presence of external magnetic fields generated by permanent magnets.

II. MATERIALS AND METHODS

A. Materials

Two types of magnetic suspensions were employed in this work: FFs and MRFs. Three oil-based FFs were purchased from Ferrotec (APG series). The particulate material in these FFs is magnetite (9 nm average diameter) at a total loading of approximately 5% by volume as determined by fitting a log-normal probability function to the size distribution and using a Langevin-like magnetization dependence following the methodology suggested by Chantrell *et al*. (1978). The FFs employed have the same magnetization dependence on the field strength, $M(H)$, and therefore exhibit the same magnetic response under a given external magnetic field. The saturation magnetization of the FFs is 24.8 ± 0.7 kA/m.

Their interfacial properties (at the liquid/air interface) are also similar, and according to the manufacturer, the surface tension at 25 °C is approximately 33 mN/m.

FFs remain kinetically stable against aggregation and sedimentation over a period of months. The main difference between the FFs used is their shear viscosity. Steady shear measurements in the absence of a magnetic field, using a plate-plate geometry (20 mm diameter and 300 μm gap) in a Physica MCR501 rheometer (Anton Paar) at 18.8 °C (the

[1]Cambridge Polymer Group, I, "The capillary breakup extensional rheometer (CaBER^{TM})," http://www.campoly.com/files/3913/7122/7764/007_New.pdf (Accessed in November, 2014).

temperature at which the extensional experiments were carried out) gave constant viscosities of 133, 349, and 743 mPa·s for FF100, FF200, and FF500, respectively (Fig. 2). As expected, the effect of the superposition of a magnetic field perpendicular to the flow field was negligible in the rheological response with changes in the shear viscosity within the experimental error.

The MRF employed in this work was graciously supplied by Lord Corporation (MRF-132). The main particulate material is a micron-sized quasispherical carbonyl iron at a particle loading of 32 vol. %. The presence of fumed silica, organoclays, and surfactants in solution is also possible, but the exact composition of this MRF is unknown because it is proprietary. The MRF is formulated in a hydrocarbon oil and according to the manufacturer, the density of the MRF is around 3000 kg/m^3. The surface tension of the MRF is approximately 50 mN/m [Ewoldt *et al.* (2011)].

In the absence of magnetic fields, the steady shear viscosity of the MRF is a strongly decreasing function of the shear rate (shear thinning behavior). When an external magnetic field is applied perpendicularly to the flow streamlines, the shear viscosity increases (especially at low shear rates) and for large enough fields an apparent yield stress can be observed, as found by de Vicente *et al.* (2011a). Due to the large density mismatch between the iron particles and the carrier fluid, these MRFs sediment over time (in a few days). However, preliminary measurements in a Turbiscan Classic (Formulaction) demonstrate that within the time scale employed in this work, the MRF remains stable and does not appreciably sediment at rest.

Additional fluid properties for the FFs and MRF are shown in Table I, where ρ is the density, Γ is the surface tension, Ms is the fluid saturation magnetization, χ is the initial susceptibility, ϕ is the magnetic particle concentration, σ is the dispersity of the particle size given by its standard deviation, and d is the average particle size.

B. Methods

In order to perform rheological characterization of the extensional behavior of magnetic suspensions in the CaBER 1^{TM} device under the influence of an external homogeneous

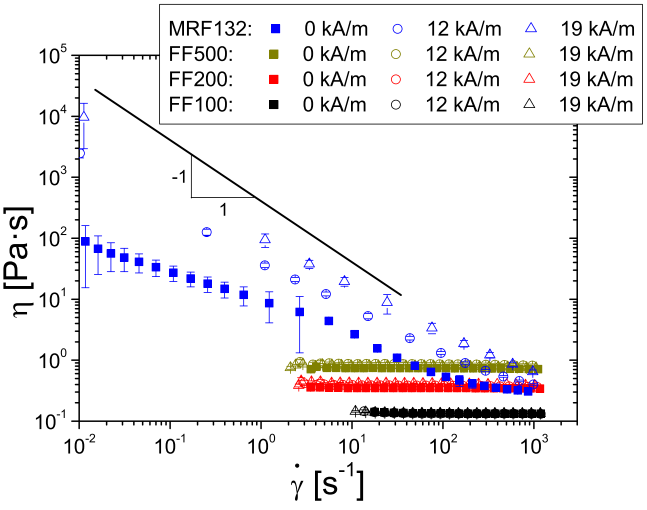

FIG. 2. Steady shear viscosity curves measured at 18.8 °C. Variation of the shear viscosity with the intensity of the applied magnetic field perpendicular to the shear flow. The error bars at each point represent the corresponding standard deviation from three independent measurements with fresh samples. The black solid line is a guiding line with slope −1 added for the sake of clarity.

TABLE I. Fluid properties at 25 °C with no magnetic field.

	FF100[a,b]	FF200[a,b]	FF500[a,b]	MRF-132
ρ (kg/m^3)	1120	1050	1060	∼3000[a]
Γ (mN/m)	∼33[c]	∼33[c]	∼33[c]	∼50[d]
Ms (kA/m)	25.5	24.3	24.5	[e]
χ (-)	0.5933	0.6152	0.5325	[e]
ϕ (vol. %)	5.7	5.4	5.4	32[a]
σ (nm)	0.25	0.2	0.28	[e]
d (nm)	8.98	9.52	8.59	1000[a]

[a]As provided by the manufacturer.
[b]Further details on the physical properties of the ferrofluids investigated in this work are given in Andablo-Reyes (2010).
[c]Surface tension values at 25 °C, interpolated from the curve of surface tension vs. temperature provided by the manufacturer. The effective surface tension of FFs at 18.8 °C will be slightly larger than this value.
[d]Estimated from Ewoldt *et al*. (2011).
[e]Information not available from the manufacturer.

magnetic field, we have developed two types of fixtures, one generating a magnetic field aligned with the extensional flow undergone by the fluid sample (*parallel configuration*[2]) and another with a magnetic field oriented perpendicularly to the extensional flow (*perpendicular configuration*). Both fixtures consist of a scaffold structure made of Polyoxymethylene (POM), a nonmagnetic thermoplastic material typically used in precision parts requiring excellent dimensional stability, adapted to the available space in the CaBER 1^{TM} device. The fixtures hold four rodlike permanent magnets centered at the corners of a square base with the fluid sample located at the center of symmetry of the prism as shown in Fig. 3. In both the parallel and perpendicular configurations, the light beam can travel undisturbed from the light source to the light detector and through the sample, and the recording of the filament thinning process by a video camera placed at the front is also allowed. Moreover, in both configurations, neodymium (NdFeB) rod magnets with nickel-plated (Ni-Cu-Ni) coating were used (Supermagnete). The main differences between the two fixtures are in the orientation, length, and magnetization of the magnet rods (N40 for the parallel configuration and N42 for the perpendicular configuration), which result in different intensities of the generated magnetic field. More details about the design of these fixtures can be found in the Supplementary Material.

The magnetic fields generated in both fixtures were measured along the *x*, *y*, and *z*-directions using a planar Hall probe (F.W. BELL 5100 SERIES) connected to a 5170 Gauss/Tesla meter without the rheometer plates in place,[3] and the results are plotted in Fig. 4. It can be observed that the parallel configuration generates a more homogeneous, but less intense, magnetic field along the direction of the extensional flow (*z*-direction) than the perpendicular configuration. This difference in the homogeneity of the magnetic field is related directly to the length of the magnets, i.e., the longer the magnetic rods are,

[2]The parallel configuration operating with four electromechanical solenoids is shown in the Supplementary Material. This configuration is currently under development.
[3]In spite of the fact that a planar Hall probe was used for this purpose, it was not possible to measure the field in the presence of the rheometer plates due to space limitation. Nevertheless, these plates are made of an aluminum alloy (AlMgSi1), having less than 0.5% of Fe in its composition, and a relative permeability of 1 [Eskelinen *et al*. (2004)]. Thus, the influence of the rheometer plates is negligible and a substantial distortion of the magnetic field lines is not expected to occur when the plates are in place.

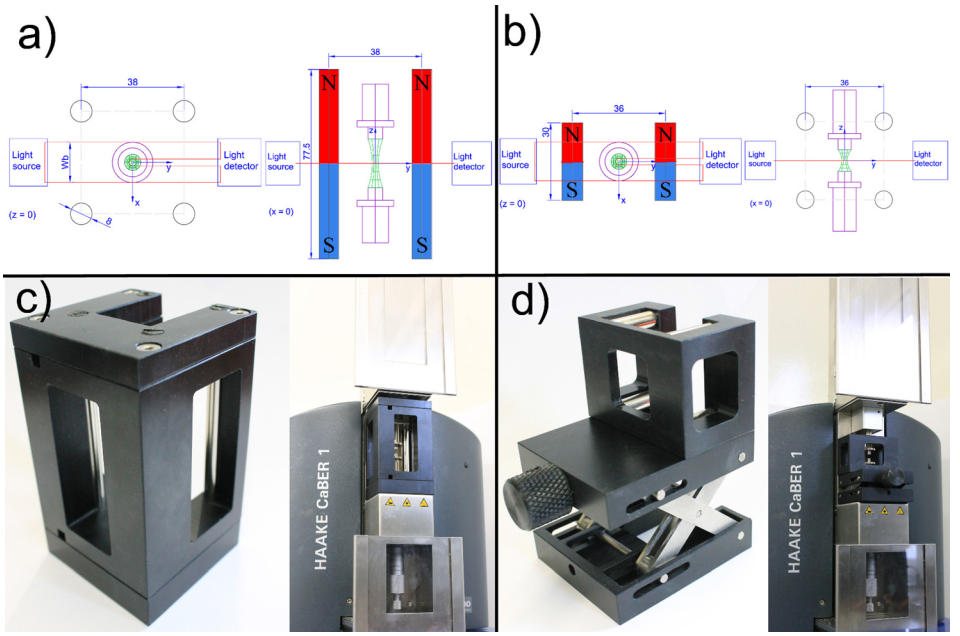

FIG. 3. Top and front views of a sketch of the scaffold structures adapted to a CaBER 1™ device and holding four rodlike permanent magnets designed for the parallel (a) and perpendicular (b) configurations (dimensions in mm); pictures of the embodiments of the fixtures for the parallel (c) and (d) perpendicular configurations.

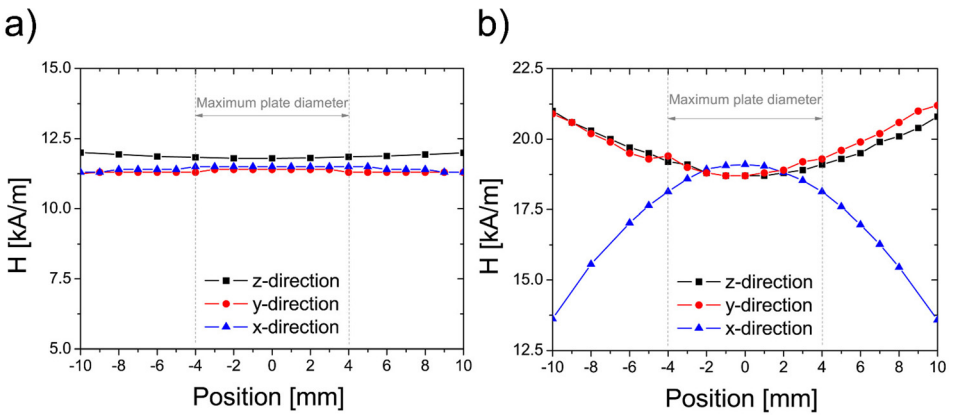

FIG. 4. Experimental measurements of the variation of the intensity of the magnetic field (H) in the x, y, and z-directions for the parallel (a) and perpendicular (b) configurations. The magnets are oriented in z-direction and x-direction for the parallel and perpendicular configurations, respectively. The extensional flow occurs in z-direction for both configurations. The light gray dashed lines represent the contour of the maximum sized initial filament, corresponding to the 8 mm plate. The lines between the points are simply a guide to the eye.

TABLE II. Experimental values of the average and standard deviation of the intensity of the magnetic field (H in kA/m) generated in both configurations along x, y, and z-directions for the maximum fluid sample volume possible in the CaBER 1™ device.

	Parallel configuration	Perpendicular configuration
x-direction	11.5 ± 0.1	18.7 ± 0.4
y-direction	11.4 ± 0.1	18.9 ± 0.3
z-direction	11.9 ± 0.1	19.6 ± 0.7

the more homogeneous the magnetic field is in the neighborhood of its plane of symmetry. Table II shows the mean and standard deviation values of the intensity of the magnetic fields generated in both configurations along the axes for the maximum fluid sample volume possible in the CaBER, i.e., a cylindrical filament of 20 mm length (z-direction) and 8 mm diameter (xy-plane). It must be noted that this is the worst case scenario, as the actual filament size during the CaBER experiment would be smaller. This ensures the homogeneity of the magnetic field within the fluid sample with a deviation smaller than 5% for both fixtures. More details about the homogeneity of the magnetic field are reported in the Supplementary Material.

The time evolution of the diameter of the filament at the midpoint was measured using the laser micrometer available in the CaBER 1^{TM} device for three different FFs and one MRF. Initially, these fluids were characterized without any magnetic field applied, and subsequently under the influence of external magnetic fields with different intensities and orientations. Before each set of measurements, the laser micrometer was calibrated. The calibration curve of the laser micrometer is linear even for low voltages, thus diameters as low as 5 μm can be measured in practice, but the calibrated resolution of the sensor is up to 20 μm. [Anna and McKinley (2001)]. All the filament thinning experiments were carried out at $18.8 \pm 0.6\,^{\circ}$C. The temperature of the plates was controlled with a thermal bath (Haake C/DC Refrigerated Circulators K15) and the actual temperature of the fluid placed between the plates of the CaBER 1^{TM} device was measured with a thin thermocouple with fast response (Weller sensor thermocouple, type K, 0.1 mm diameter) connected to a multimeter (Agilent Technologies, U1272A).

Since the rheological properties of colloidal suspensions may depend on the dispersion quality [Galindo-Rosales *et al.* (2011)], fresh samples were always used for each measurement after being redispersed in an ultrasound bath (Velleman VTUSC3) for 300 s. The 4 mm diameter plates were chosen and an initial gap between the plates (h_0) of 1.5 mm was fixed. The final axial separation between the plates (h_f) was fixed at 5.3 mm, and the initial stretch profile was linear with a "strike time" of 20 ms. The experimental protocol was kept independent of the orientation of the imposed magnetic field. The sample aspect ratio is given by $\Lambda(t) = [h(t)/2R_0]$, where $h(t)$ is the distance between the endplates. The initial aspect ratio is $\Lambda_0 = (h_0/2R_0)$ and plays an important role in order to ensure that capillary break-up rheometry yields reliable and successful results. It is required that $h_0/l_{\text{cap}} < 1$, where $l_{\text{cap}} = \sqrt{(\Gamma/\rho g)} \sim 1.8$ mm is the capillary length, to ensure that the interfacial force arising from surface tension is capable of supporting the liquid bridge against the sagging induced by the gravitational body force. Only in this way is the initial sample approximately cylindrical, and the initial deformation results in a top-bottom symmetric deformation with the formation of an axially uniform filament when the top plate reaches the final position. Numerical simulations for filament stretching rheometry [Yao and McKinley (1998)] suggest that Λ_0 would be optimal in the range $0.5 \leq \Lambda_0 \leq 1$. The final aspect ratio $\Lambda_f = h_f/2R_0$ is attained when the plates are completely separated and controls the total Hencky strain[4] that is applied to the sample. It neither has any influence on the measurement of the relaxation time in the case of viscoelastic fluids [Rodd *et al.* (2005)], nor on the time evolution of the diameter and curvature at the neck for a yield stress fluid [Niedzwiedz *et al.* (2009)]. Since we were operating with permanent magnets, the sample was initially loaded between the plates of the CaBER 1^{TM} device, and only then the magnetic fixture was placed in position, and finally the

[4]The Hencky strain is defined as $\varepsilon = \ln(h_f/h_0)$.

experiment was triggered; this was done so that the presence of the magnetic field would not complicate the loading of the sample into the rheometer.

Although the analysis of filament thinning experiments assumes top-bottom symmetry about the midplane, gravitational effects break this symmetry and lead to a weak axial flow downwards. In practice this leads to some degree of sagging of the filament such that after breakup, more than half of the initial volume of fluid is found at the lower plate [Anna and McKinley (2001)]. In order to quantify the effect of sagging compared with the opposing capillary forces, we refer to the Bond number ($Bo = (\rho g D_0^2/4\Gamma)$) that compares the gravitational force with the surface tension force. Even for the smaller plate supplied with the CaBER 1^{TM} device, $Bo > 1$ as a result of the large density of the fluids, thus some top-bottom asymmetry was readily observable before the filament breakup event. However, it is known that the extent of this axial drainage depends not only on the magnitude of the Bond number but also on the total time that the liquid bridge remains connected. Thus, it is expected that under the influence of a magnetic field, this sagging effect may be reduced by the presence of induced magnetic field body forces in the fluids. In order to check whether the orientation of the polarity of the magnetic field has any effect on the filament sagging, we have performed experiments with the two orientations of the magnets for the parallel configuration. Finally, we have also recorded the filament thinning process using a high speed video camera (Photron FASTCAM Mini UX100) at 5000 fps. The image analysis allowed us to assess the influence of gravity and inertia on the CaBER experiments.

The experimental results presented and discussed in Sec. III are the result of averaging at least three independent experiments.

III. RESULTS AND DISCUSSION

The experimental results obtained by the CaBER 1^{TM} device for all FFs tested (FF100, FF200, and FF500) are shown in Fig. 5 (diameter measured using the laser and sensor), Fig. 6 (filament thinning process recorded with a high-speed camera), and Fig. 7 (comparison between the measurements carried out with laser and high-speed camera). In all these figures, the initial time ($t = 0$) corresponds to the start of the movement of the upper plate.

As shown in Fig. 5,without an applied magnetic field, the diameter of the thinning filament decays linearly in time prior to breakup, a characteristic behavior of Newtonian fluids. Moreover, since the necking driven by the surface tension is exclusively balanced by the viscous resistance, the higher the shear viscosity of the sample, the larger the break-up time in the CaBER tests and the clearer this purely viscous behavior is observed. The results obtained with the laser and the high-speed camera are in agreement with the behavior observed in conventional Newtonian fluids (Fig. 6) [Campo-Deaño and Clasen (2010]. For the less viscous fluid (FF100), gravitational and inertial effects are significant and the measurements using the laser showed a final bump due to the filament vertical asymmetry, which can be corrected in data analysis from the images obtained using the high-speed camera (Fig. 7).

It can also be observed from Fig. 5 that when the magnetic field is applied perpendicularly to the extensional flow direction, the time evolution of the mid-diameter is also linear, again corresponding to a Newtonian fluid. Moreover, the slope only changes marginally from the value observed when no magnetic field is applied. The presence of an external magnetic field perpendicularly oriented to the flow direction reduces the break-up time of the filament, although this effect is more evident for the larger shear viscosity samples. It can be inferred that this is a consequence of having the magnetic particles of the fluid

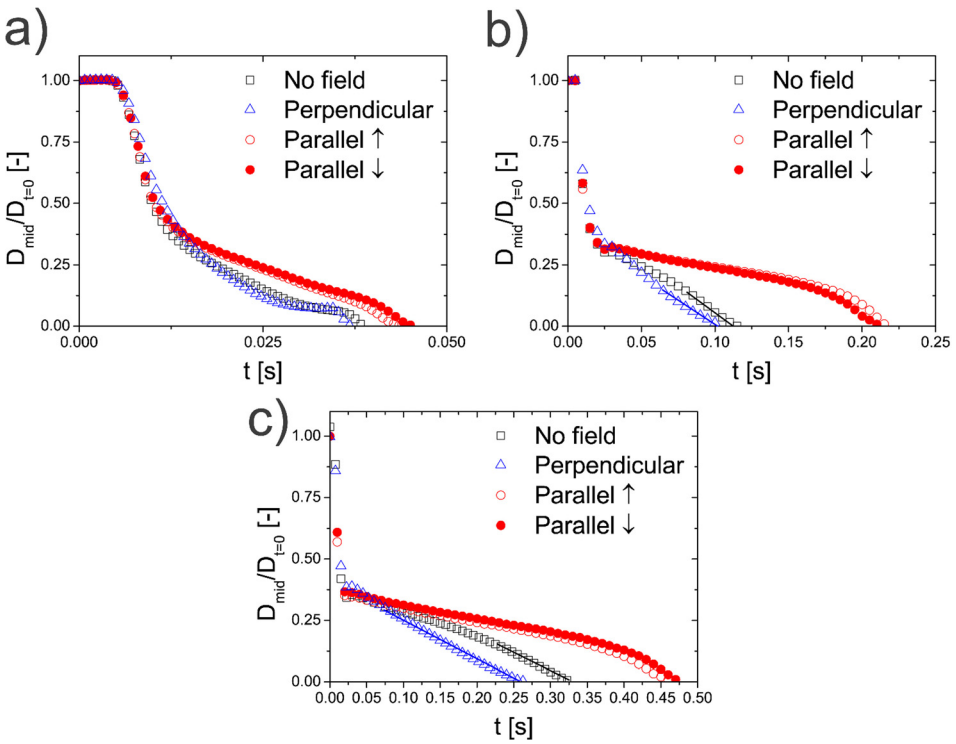

FIG. 5. Effect of the magnetic field on the time evolution of the mid-diameter for each FF measured with the laser micrometer incorporated in the CaBER 1^{TM} device: (a) FF100, (b) FF200, and (c) FF500. Guide lines are added to show the linear dependency of the time evolution of the mid-diameter for no magnetic field (solid line fitted to square symbols) and perpendicular configuration (solid line fitted to triangles).

forming chains that are oriented perpendicularly to the flow direction, resulting in a more brittle behavior of the filament. This result was also confirmed by the high-speed videos (Fig. 6). These results show that elongational experiments are more sensitive to subtle changes in the microstructure of the fluid than steady shear measurements (Fig. 2), where no noticeable differences were observed. It is important to emphasize that this comparison is just regarding the flow field, i.e., elongational flow versus simple shear flow, as the magnetic field remains perpendicular for both set of experiments.

Finally, when the magnetic field was applied parallel to the flow direction, the filament lasted longer than in the two previous configurations, i.e., under no magnetic field and under perpendicular magnetic field. These results are consistent with previous experimental results obtained by Timko and coworkers [Sikora *et al*. (2010); Habera *et al*. (2013)], who analyzed the influence of magnetic field on the breakup of a FF jet. They observed an elongation of the neck so that a drop separates at a larger distance from the nozzle with increasing parallel magnetic field, whereas in a perpendicular magnetic field the corresponding neck length was nearly independent of the magnetic field strength. When the magnetic field is aligned with the flow direction, the magnetic particles are also aligned with the fluid flow and the magnetic body forces acting as a result of their magnetization counterbalance the effect of the surface tension more effectively than in the perpendicular configuration. This results in a longer filament thinning process, an indication of a higher effective viscosity. As the filament progressively thins, the strength of the magnetic body force ($\propto L^3$) decreases more than that of the surface forces ($\propto L^2$) and as a consequence the contribution

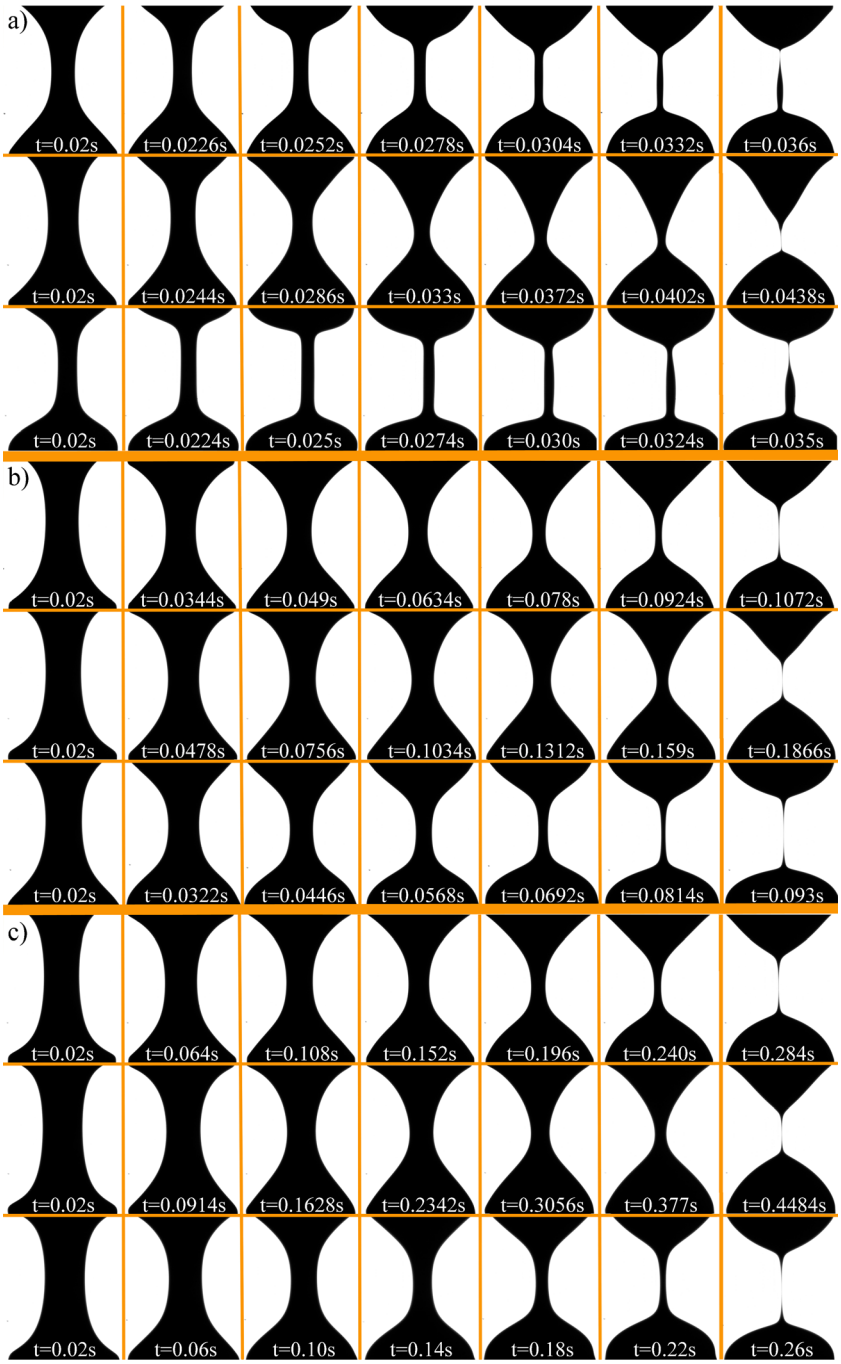

FIG. 6. Filament thinning process recorded with a high speed camera at 5000 fps for no magnetic field (first row), parallel configuration (second row), and perpendicular configuration (third row): (a) FF100, (b) FF200, and (c) FF500.

of magnetic force at the neck becomes negligible in the final stages of thinning and the filament breaks as if there was no magnetic field applied.

It is important to highlight here that the orientation of the external magnetic field with regards to the flow direction has a more pronounced effect on the extensional behavior of

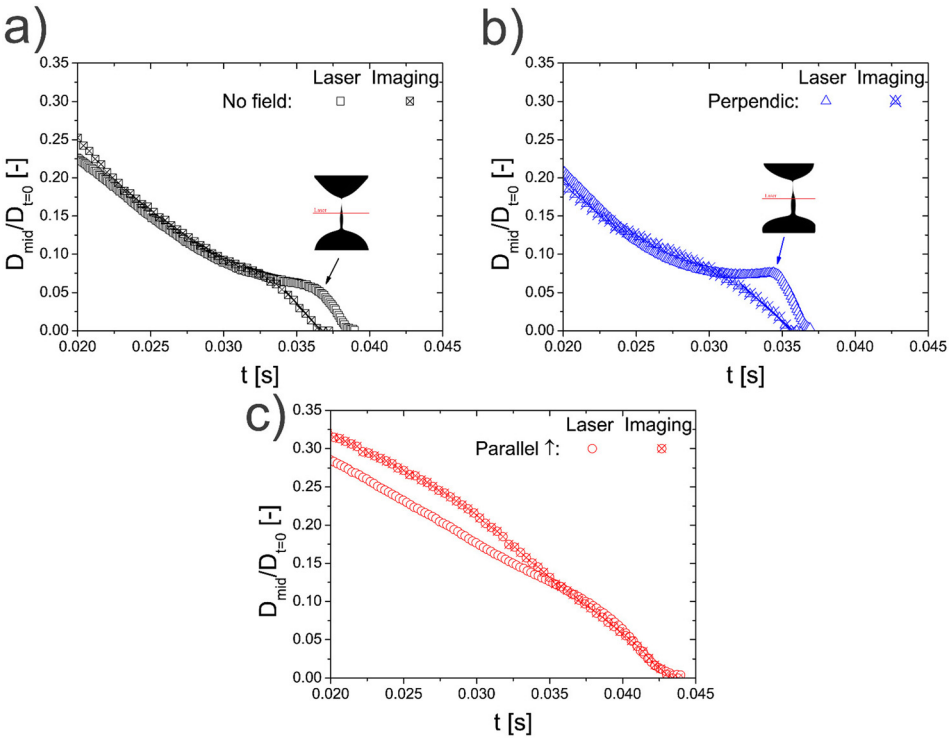

FIG. 7. Comparison between the time evolution of the diameter of FF100 as measured with the laser and calculated from the image processing at the thinnest point of the filament: (a) No magnetic field, (b) perpendicular configuration, and (c) parallel configuration. Solid guide lines are added to show the linear dependency of the time evolution of the mid-diameter for no magnetic field and perpendicular configuration.

the FFs than the intensity of the field, since the intensity of the magnetic field generated by the parallel magnet's configuration (∼12 kA/m) was smaller than the intensity of the magnetic field generated by the perpendicular configuration (∼19 kA/m).

Figure 8 shows the influence of the magnetic field on the time evolution of the mid-diameter for the MRF measured with the laser incorporated in the CaBER 1^{TM} device. The changes observed in the rheological response are more dramatic that in the case of the FFs, due to the larger particle size and concentration of the MRF. Under the influence of an external magnetic field, the MRF behaves like a solid. When the magnetic field is perpendicular to the flow direction, the particles aggregate in horizontal chains and the vertical extensional flow of the liquid results in a shear process relative to the MRF particles that result in the filament yielding quickly like a plastic material. Since the MRF turns into a solidlike material as soon as the perpendicular magnetic field is applied, the filament is already broken by the time the top plate reaches the final height.

In the case of a parallel magnetic field, the chains are aligned with the flow direction and the fluid ends up forming a solid bridge between both plates because the filament resistance strength is in the direction of the imposed flow. The magnetic forces introduced by the particles chains aligned with the flow direction are stronger than the surface tension and the filament does not breakup. Figures 9(a) and 9(b) show the shape of the filament in two perpendicular views after the experiment with the applied parallel magnetic field. The filament maintains its shape and does not break as long as the magnetic field is applied. Different final heights (h_f) were also tested, but the fluid filament never broke up even for $h_f = 15$ mm. It can also be noticed that even though the shape of the filament is

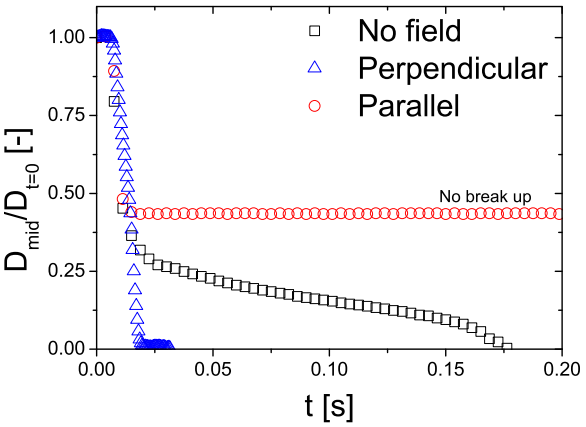

FIG. 8. Effect of the magnetic field on the time evolution of the mid-diameter for the MRF fluids measured with the laser incorporated in the CaBER 1^{TM} device.

axisymmetric relative to the z-axis, gravity effects are not negligible. Figures 9(c) and 9(d) show the corresponding shape of the broken filament obtained with the perpendicular magnetic field. In this case the filament broke as a solid, and its final shape is clearly not axisymmetric, but symmetric relative to the $z = 0$ plane. We note that these final shapes will last as long as the magnetic field, either parallel or perpendicular, is applied.

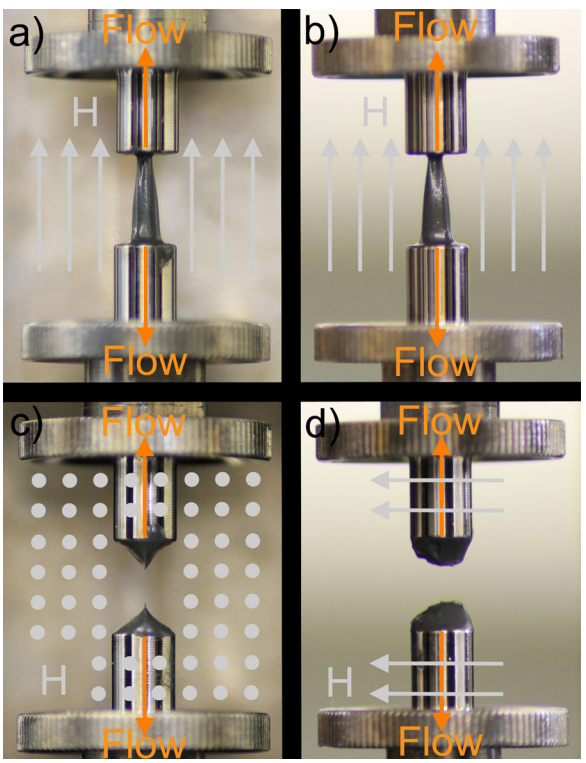

FIG. 9. Effect of the magnetic field on the filament of the MRF: (a) and (b) Front and side views for the case of an applied external magnetic field parallel (∼12 kA/m) to the flow, respectively; (c) and (d) front and side views for the case of an applied external magnetic field perpendicular (∼19 kA/m) to the flow, respectively.

IV. CONCLUSIONS AND FINAL REMARKS

In this work, we characterized magnetic fluids (three FFs and one MRF) under extensional flow using capillary thinning experiments carried out with the CaBER 1^{TM} device using appropriate fixtures. Three different test configurations have been considered: No magnetic field, magnetic field perpendicular to the extensional flow direction, and magnetic field parallel to the flow. Two types of fixtures were developed in order to generate the magnetic field corresponding to these latter two configurations. The FFs exhibited Newtonian behavior when no magnetic field was supplied, and the application of a perpendicular magnetic field did not change this response significantly. However, when the external magnetic field was aligned with the extensional flow direction, the induced magnetic body forces were able to hold the filament in place over a longer period of time, which resulted in a higher effective viscosity. Therefore, the extensional behavior of FFs strongly depends on the orientation of the magnetic field, in contrast to their behavior under shear where the viscosities of the FFs tested do not change significantly under the presence of the magnetic field. The MRF also exhibited different extensional behavior depending on the orientation of the applied external magnetic field, i.e., yielding like a plastic material when the magnetic field was perpendicular to the flow and creating a permanent bridge of fluid between the plates when the magnetic field was aligned with the flow direction. These results are consistent with former experiments and theoretical predictions concerning chain formation in FFs, but more experiments are required to provide an extensive database compiling the effects of fluid composition, magnetic field strength, and orientation on the extensional behavior of FFs to enable a detailed theoretical description. Nevertheless, the set of fixtures developed for the CaBER 1^{TM} device opens the possibility of using capillary thinning experiments for magnetic suspensions allowing their rheological characterization under elongational flow. Future work will focus on a detailed image analysis of the filament thinning process, and a new set of experiments with different intensities of the applied magnetic field and different magnetic fluids in order to provide a solid data-set for a better understanding of these complex smart materials under extensional flow.

ACKNOWLEDGMENTS

The authors acknowledge funding from Fundação para a Ciência e a Tecnologia (FCT), COMPETE, QREN, and European Union (FEDER) through Project No. PTDC/EQU-FTT/113811/2009 and FCT Investigator Grant No. IF/00190/2013; MINECO through Project Nos. MAT2010-15101 and MAT2013-44429-R; Junta de Andalucía through Project Nos. P10-RNM-6630 and P11-FQM-7074; and the Spanish Ministry of Science and Innovation (FPU program) through the pre-doctoral fellowship AP2008-02138. L. Campo-Deaño is acknowledged for her selfless help in taking all the pictures and videos with the high-speed camera and also for fruitful discussions. The Authors would also like to acknowledge Arif Zainuddin Nelson for having proofread the manuscript graciously.

References

Andablo-Reyes, E. A. (2010). Thin film rheology and ferrohydrodynamic lubrication of magnetic fluids. Ph.D. thesis, Universidad de Granada, Spain.

Anna, S. L., C. Rogers, and G. H. McKinley, "On controlling the kinematics of a filament stretching rheometer using a real-time active control mechanism," J. Non-Newtonian Fluid Mech. **87**, 307–335 (1999).

Anna, S. L., and G. H. McKinley, "Elasto-capillary thinning and breakup of model elastic liquids," J. Rheol. **45**, 115–138 (2001).

Anna, S. L., G. H. McKinley, D. A. Nguyen, T. Sridhar, S. Muller, J. Huang, and D. F. James, "An interlaboratory comparison of measurements from filament-stretching rheometers using common test fluids," J. Rheol. **45**(1), 83–114 (2001).

Bazilevsky, A., V. Entov, and A. Rozhkov, "Liquid filament microrheometer and some of its applications," in *Proceedings of the Third European Rheology Conference and Golden Jubilee Meeting of the British Society of Rheology*, edited by D. R. Oliver (Springer, Netherlands, 1990), pp. 41–43.

Bose, H., T. Gerlach, and J. Ehrlich, "Magnetorheological torque transmission devices with permanent magnets," J. Phys.: Conf. Ser. **412**, 012050 (2013).

Bossis, G., O. Volkova, S. Lacis, and A. Meunier, "*Magnetorheology: Fluids, Structures and Rheology*," in *Ferrofluids: Magnetically controllable fluids and their applications*, Lecture notes in Physics, 594, 202–230 edited by S. Odenbach (Springer-Verlag, Berlin, Heidelberg, 2002).

Braithwaite, G. J. C., S. H. Spiegelberg, and G. H. McKinley, "Apparatus and methods for measuring extensional rheological properties of a material," US Patent No. US006711941B2 (2002).

Campo-Deaño, L., and C. Clasen, "The slow retraction method (SRM) for the determination of ultra-short relaxation times in capillary breakup extensional rheometry experiments," J. Non-Newtonian Fluid Mech. **165**, 1688–1699 (2010).

Chantrell, R. W., J. Popplewell, and S. W. Charles, "Measurements of particle size distribution parameters in ferrofluids," IEEE Trans. Magn. **14**, 975–977 (1978).

Chellamuthu, M., E. M. Arndt, and J. P. Rothstein, "Extensional rheology of shear thickening nano particle suspensions," Soft Matter **5**, 2117–2124 (2009).

de Gans, B. J., H. Hoekstra, and J. Mellema, "Non-linear magnetorheological behaviour of an inverse ferrofluid," Faraday Discuss. **122**, 209–224 (1999).

de Vicente, J., "Magnetorheology: A review," e-rheo-iba **1**, 1–18 (2013). Available at http://www.e-rheo-iba.org/Papers/V01P01-Pub.pdf.

de Vicente, J., D. J. Klingenberg, and R. Hidalgo-Álvarez, "Magnetorheological fluids: A review," Soft Matter **7**, 3701–3710 (2011a).

de Vicente, J., J. A. Ruiz-López, E. Andablo-Reyes, J. P. Segovia-Guitérrez, and R. Hidalgo-Álvarez, "Squeeze flow magnetorheology," J. Rheol. **55**, 753–779 (2011b).

Eskelinen, H., J. Heinola, and P. Silventoinen, *DFM(A)-Aspects for a Microwave Waveguide Ring Resonator Design* (Tutkimusraportti/Lappeenrannan teknillinen yliopisto, Konetekni-ikan Osasto, Lappeenranta University of Technology, Finland, 2004).

Ewoldt, R. H., P. Tourkine, G. H. McKinley, and A. E. Hosoi, "Controllable adhesion using field-activated fluids," Phys. Fluids **23**, 073104 (2011).

Galindo-Rosales, F. J., M. A. Alves, and M. S. N. Oliveira, "Microdevices for extensional rheometry of slow viscosity elastic liquids: A review," Microfluid. Nanofluid. **14**, 1–19 (2013).

Galindo-Rosales, F. J., P. Moldenaers, and J. Vermant, "Assessment of the dispersion quality in polymer nanocomposites by rheological methods," Macromol. Mater. Eng. **296**(3-4), 331–340 (2011).

Gerlach, T., J. Ehrlich, and H. Bose, "Novel active vibration absorber with magnetorheological fluid," J. Phys.: Conf. Ser. **149**, 012049 (2009).

Gonçalves, F. D., and J. D. Carlson, "An alternative operation mode for MR fluids-magnetic gradient pinch," J. Phys.: Conf. Ser. **149**, 012050 (2009).

Guo, C. Y., X. Gong, S. Xuan, Q. Yan, and X. Ruan, "Squeeze behavior of magnetorheological fluids under constant volume and uniform magnetic field," Smart Mater. Struct. **22**, 045020 (2013a).

Guo, C. Y., X. L. Gong, S. H. Xuan, L. J. Qin, and Q. F. Yan, "Compression behaviors of magnetorheological fluids under nonuniform magnetic field," Rheol. Acta **52**, 160–176 (2013b).

Habera, M., M. Fabian, M. Svikova, and M. Timko, "The influence of magnetic field on free surface ferrofluid flow," Magnetohydrodynamics **49**(3–4), 402–406 (2013). Available at http://mhd.sal.lv/contents/2013/3/MG.49.3.28.R.html.

Haward, S. J., A. Jaishankar, M. S. N. Oliveira, M. A. Alves, and G. H. McKinley, "Extensional flow of hyaluronic acid solutions in an optimized microfluidic cross-slot device," Biomicrofluidics **7**, 044108 (2013).

Huang, J., J. Zhang, Y. Yang, and Y. Wei, "Analysis and design of a cylindrical magnetorheological fluid brake," J. Mater. Process. Technol. **129**, 559–562 (2002).

Jacob, R., "Magnetic fluid torque and force transmitting device," US Patent No. 2,575,360 (1951).

Laun, H. M., C. Kormann, and N. Willenbacher, "Rheometry on magnetorheological (MR) fluids I: Steady shear flow in stationary magnetic fields," Rheol. Acta **35**, 417–432 (1996).

Matta, J., and R. P. Titus, "Liquid stretching using a falling cylinder," J. Non-Newtonian Fluid Mech. **35**, 215–229 (1990).

McKinley, G. H., *Visco-Elasto-Capillary Thinning and Break-Up of Complex Fluids. Rheology Reviews* (The British Society of Rheology, 2005), Vol. 3, pp. 1–48.

McKinley, G. H., O. Brauner, and M. Yao, "Kinematics of filament stretching in dilute and concentrated polymer solutions," Korea Aust. J. Rheol. **13**(1), 29–35 (2001).

Morrison, F. A., *Understanding Rheology* (Oxford University, New York, 2001).

Niedzwiedz, K., O. Arnolds, N. Willenbacher, and R. Brummer, "How to characterize yield stress fluids with capillary breakup extensional rheometry (CaBER)?," Appl. Rheol. **19**(4), 41969 (2009).

Ocalan, M., and G. H. McKinley, "High-flux magnetorheology at elevated temperatures," Rheol. Acta **52**, 623–641 (2013).

Olabi, A. G., and A. Grunwald, "Design and application of magneto-rheological fluid," Mater. Des. **28**, 2658–2664 (2007).

Rodd, L. E., T. P. Scott, J. J. Cooper-White, and G. H. McKinley, "Capillary break-up rheometry of low-viscosity elastic fluids," Appl. Rheol. **15**, 12–27 (2005).

Ruiz-López, J. A., R. Hidalgo-Álvarez, and J. de Vicente, "Continuous media theory for MR fluids in non-shearing flows," J. Phys.: Conf. Ser. **412**, 012057 (2013).

Schultz, W. W., and S. H. Davis, "One-dimensional liquid fibers," J. Rheol. **26**(4), 331–345 (1982).

Shulman, Z. P., V. I. Kordonosky, E. A. Zaltsgendler, B. M. Prokhorov, and S. Demchuk, "Structure, physical properties and dynamics of magnetorheological suspensions," Int. J. Multiphase Flow **12**, 935–955 (1986).

Sikora, M., T. Sabados, M. Svikovac, and M. Timko, "Flowing of magnetic fluid with free surface and drop formation," Phys. Procedia **9**, 194–198 (2010).

Thermo Fisher Scientific, I, Haake™ CaBER1™ product specifications (2006).

White, E. E. B., M. Chellamuthu, and J. P. Rothstein, "Extensional rheology of a shear thickening cornstarch and water suspension," Rheol. Acta **49**, 119–129 (2010).

Yao, M., and G. H. McKinley, "Numerical simulation of extensional deformations of viscoelastic liquid bridges in filament stretching devices," J. Non-Newtonian Fluid Mech. **74**, 47–88 (1998).

See supplementary material at http://dx.doi.org/10.1122/1.4902356 for a discussion of the criteria used in the design of the fixtures used in this work.